

Beamforming and hardware design for a multichannel front-end integrated circuit for real-time 3D catheter-based ultrasonic imaging.

Ira O. Wygant^a, Mustafa Karaman^b, Ömer Oralkan^a, and Butrus T. Khuri-Yakub^a

^aE. L. Ginzton Laboratory, Stanford, CA, USA;

^bElectronics Engineering Department, Işık University, Istanbul, Turkey

ABSTRACT

We are working on integrating front-end electronics with the ultrasound transducer array for real-time 3D ultrasound imaging systems. We achieve this integration by flip-chip bonding a two-dimensional transducer array to an integrated circuit (IC) that comprises the front-end electronics. The front-end IC includes preamplifiers, multiplexers, and pulsers. We recently demonstrated a catheter-based real-time ultrasound imaging system based on a 16×16-element capacitive micromachined ultrasonic transducer (CMUT) array. The CMUT array is flip-chip bonded to a front-end IC that includes a pulser and preamplifier for each element of the array. To simplify the back-end processing and signal routing on the IC for this initial implementation, only a single array element is active at a time (classic synthetic aperture (CSA) imaging). Compared with classic phased array imaging (CPA), where multiple elements are used on transmit and receive, CSA imaging has reduced signal-to-noise ratio and prominent grating lobes.

In this work, we evaluate three array designs for the next generation front-end IC. The designs assume there are 16 receive channels and that numerous transmit pulsers are provided by the IC. The designs presented are: plus-transmit x-receive, boundary-transmit x-receive with no common elements, and full-transmit x-receive with no common elements. Each design is compared with CSA and CPA imaging. We choose to implement an IC for the full-transmit x-receive with no common elements (FT-XR-NC) design for our next-generation catheter-based imaging system.

Keywords: Ultrasound, Imaging, 3D, Volumetric, Beamforming, CMUT, Integration, Electronics

1. INTRODUCTION

We are working on catheter-based real-time volumetric imaging systems based on two-dimensional capacitive micromachined ultrasonic transducer (CMUT) arrays. In these systems, we integrate the front-end electronics with the transducer array as shown in Fig. 1. This style of integration is also explored by others.^{1,2} In our design, the front-end IC contains a combination of preamplifiers, pulsers, multiplexers, and digital control circuitry. Integrated preamplifiers minimize capacitive loading of the transducer and eliminate the need to impedance match the transducer to an external system. Integrated pulsers can drive numerous transmit elements with a minimum number of cables. Multiplexing within the IC also reduces the number of connecting cables.

We recently demonstrated³ a catheter-based real-time ultrasound imaging system based on the design shown in Fig. 1. A photograph of the transducer array and front-end IC for this system is shown in Fig. 2. The front-end IC for that system provides a pulser and preamplifier for each element in the array. However, to simplify the backend processing and IC routing for this initial implementation, the system uses classic synthetic aperture (CSA) imaging; only a single element is active at a time during transmit and receive. Compared with a classic phased array (CPA) system, where multiple elements are used on transmit and receive, a CSA system has reduced signal-to-noise ratio (SNR) and increased grating lobes.

Further author information: (Send correspondence to I.O.W.)

I.O.W.: E-mail: iwygant@stanford.edu, Telephone: 1 650 723 0150

B.T.K.: E-mail: pierreky@stanford.edu, Telephone: 1 650 723 0718

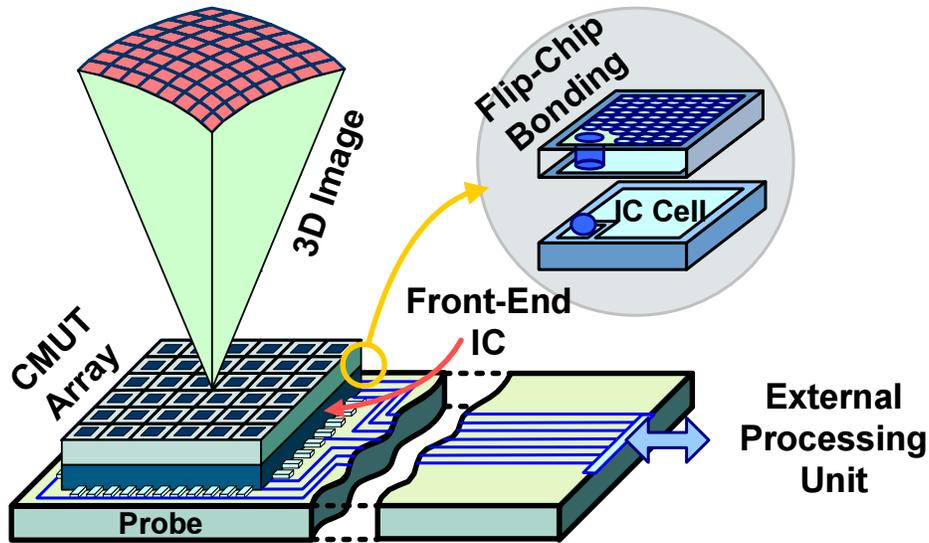


Figure 1. Design of an integrated ultrasound imaging system. A two-dimensional transducer array is flip-chip bonded an integrated circuit (IC) that comprises the front-end electronics for the system.

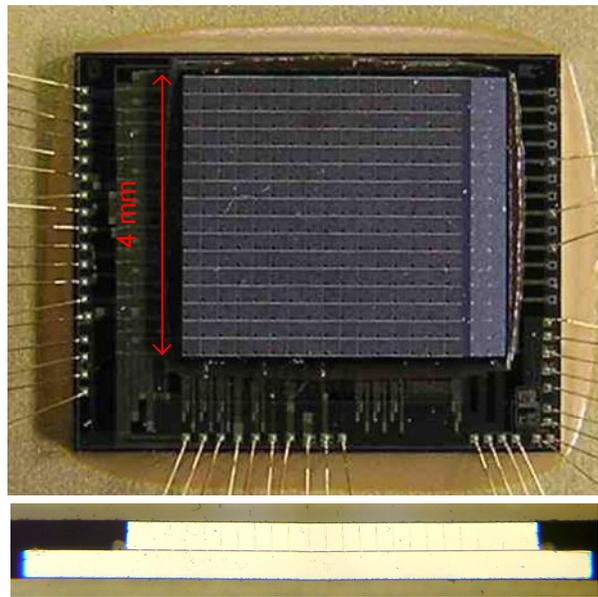


Figure 2. A two-dimensional CMUT array bonded to the initial implementation of the front-end IC. A cross section of the device is shown in the bottom picture.

The goal of this work is to design transmit and receive apertures that provide the best image quality given the hardware constraints of our system. This is the basic challenge of ultrasound array design and thus is thoroughly examined in the literature.⁶⁻¹⁰ In this paper, three designs are presented: plus-transmit x-receive (PT-XR), boundary-transmit x-receive with no common elements (BT-XR-NC), and full-transmit x-receive with no common elements (FT-XR-NC). These designs are compared with CPA and CSA imaging. The transmit array, receive array, and coarray for each design are shown in Fig. 3. Comparisons between the designs are based on their simulated 3D point spread functions, frame rates, and relative signal-to-noise ratios. We determine that the FT-XR-NC design is best-suited for the next generation of our catheter-based imaging system. A preliminary IC design for FT-XR-NC is also presented.

2. ARRAY DESIGNS

The image quality of a pulse-echo array system can be quantified by the coarray function, which corresponds to the convolution of the transmit and receive arrays.^{4,5} The far-field, continuous wave PSF of the array imaging system can be approximated by the Fourier transform of the coarray. Each sample of the coarray corresponds to a transmit-receive element combination and thus to a spatial frequency. In array design, the basic idea is to form a coarray which is minimally redundant in spatial frequency content; that is, a coarray that captures all of the spatial frequency content with a minimum number of transmit/receive pairs. The rectangular function is the coarray with no redundant spatial frequency, where each sample is generated by a single transmit-receive element pair. Apodization is another factor considered in array design. With apodization, the transmit and receive arrays are weighted to produce a desired coarray shape. For example, apodization can be used to reduce side lobes at the expense of a wider main lobe. Some array designs allow more control over the coarray through apodization than others.

Here we explore three array configurations; each one corresponds to a different tradeoff between image quality and front-end complexity. Each of the array designs is shown in Fig. 3. The 3D point spread function (PSF) for each design was simulated using Field II.¹¹ The simulated PSFs are shown in Fig. 4; plots of the one-dimensional compounded PSFs are shown in Fig. 5. The parameters used for these simulations are shown in Table 1.

Table 2 compares imaging parameters for each of the array designs. For this table, the minimum number of scan angles is calculated using the following expression.

$$Q = \frac{4Nd \sin(\theta_{max})}{\lambda} \quad (1)$$

N is the number of elements in one dimension, d is the element size, θ_{max} is the maximum scan angle, and λ is the wavelength at the upper -3 dB frequency of the transducer. Frame rate is calculated as $f_{frame} = \frac{1}{2Q^2 t_{prop}}$, where t_{prop} is the time for a single A-scan and is assumed to be 40 μ s. The factor of one half is due to the two acquisitions needed to acquire data for 32 receive elements with a 16-channel data acquisition system. Beam width is obtained from the 1D compounded PSF plot shown in Fig. 5. Image SNR is relative to a single-element A-scan and is calculated as $SNR = N_T \sqrt{N_R}$, where N_T is the number of transmit elements and N_R is the number of receive elements.

Table 1. Field II simulation parameters.

Number of Array Elements	16×16
Element Size	120- μ m × 120- μ m
Transducer Impulse Response	5 MHz, 80% fractional bandwidth
Focal Point	15 mm

2.1. Classic Phased Array (CPA) and Classic Synthetic Aperture (CSA)

CPA and CSA imaging are at opposing ends of the tradeoff between image quality and hardware complexity. CPA imaging utilizes all of the elements on transmit and receive. It provides the best possible image quality for a given array. However, for large arrays, it is difficult to implement in hardware because of the large number of active elements. The challenge of array design is to achieve image quality approaching that of CPA with reduced hardware complexity.

In CSA, a single element is used at a time for transmit and receive. Thus, only a single hardware channel is needed. The major drawbacks of CSA are low SNR and grating lobes that appear at roughly half the angle at which they appear in phased array imaging.

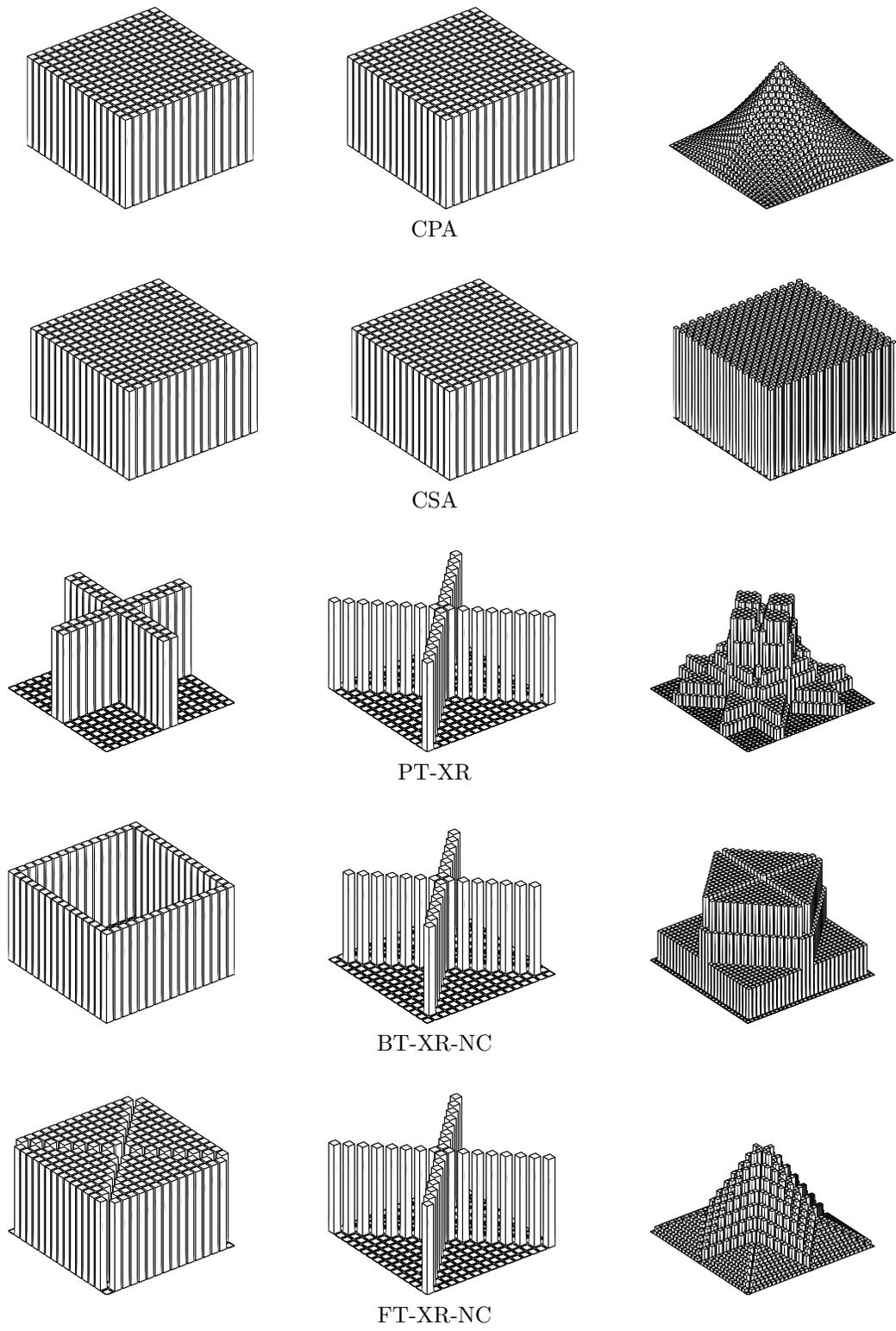


Figure 3. Array designs for a 16×16 -element array. *Column-1:* Transmit array. *Column-2:* Receive array. *Column-3:* Coarray (convolution of transmit and receive arrays).

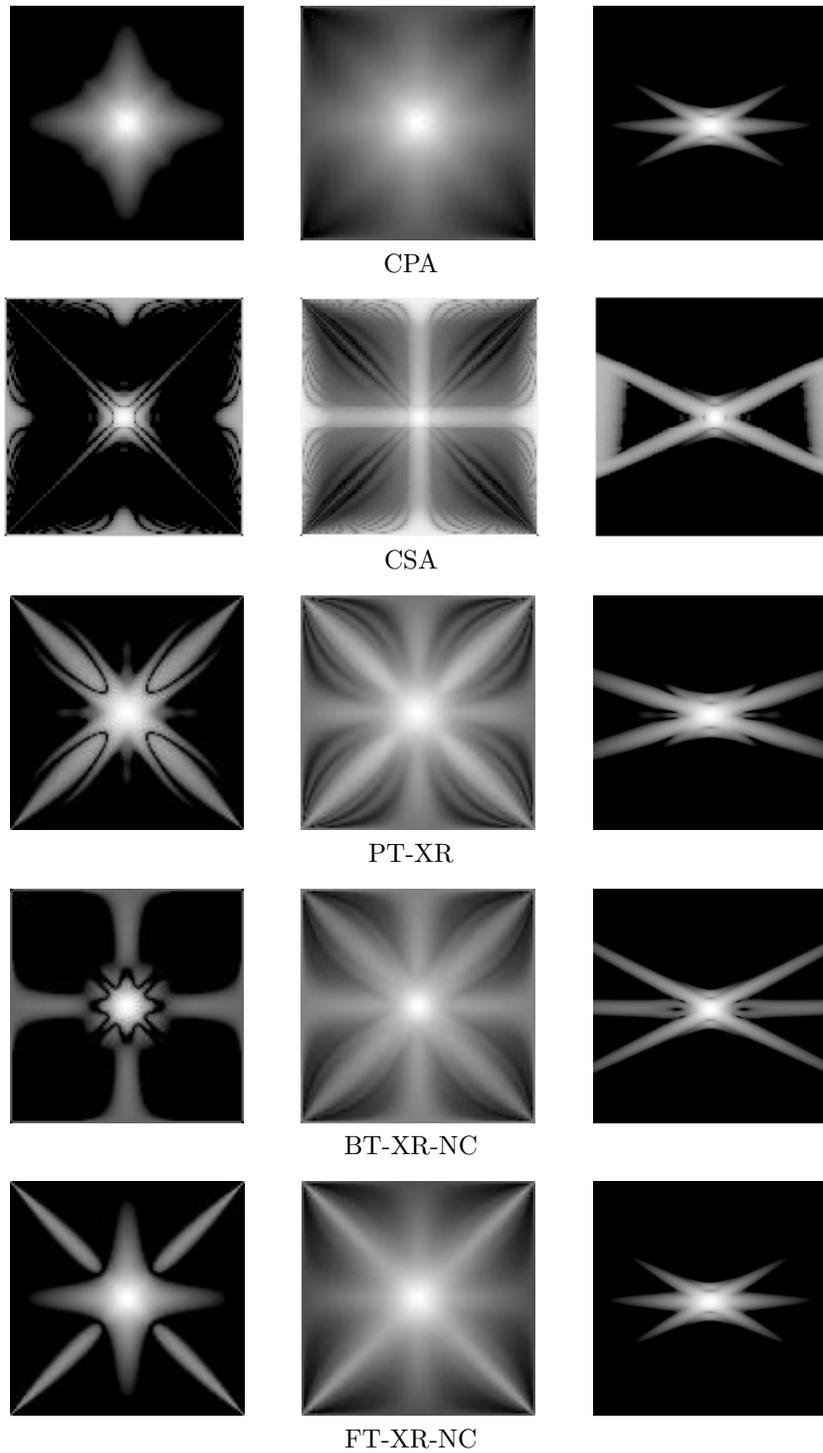


Figure 4. Simulated PSFs shown with 50 dB dynamic range. *Column-1:* C-scan with horizontal axis $\sin\theta$ ($-1 \leq \sin\theta \leq 1$) and vertical axis $\sin\phi$ ($-1 \leq \sin\phi \leq 1$). *Column-2:* Compounded C-scan with horizontal axis $\sin\theta$ ($-1 \leq \sin\theta \leq 1$) and vertical axis $\sin\phi$ ($-1 \leq \sin\phi \leq 1$). *Column-3:* B-scan with horizontal axis $\sin\theta$ ($-1 \leq \sin\theta \leq 1$) and vertical axis ρ ($13\text{mm} \leq \rho \leq 17\text{mm}$).

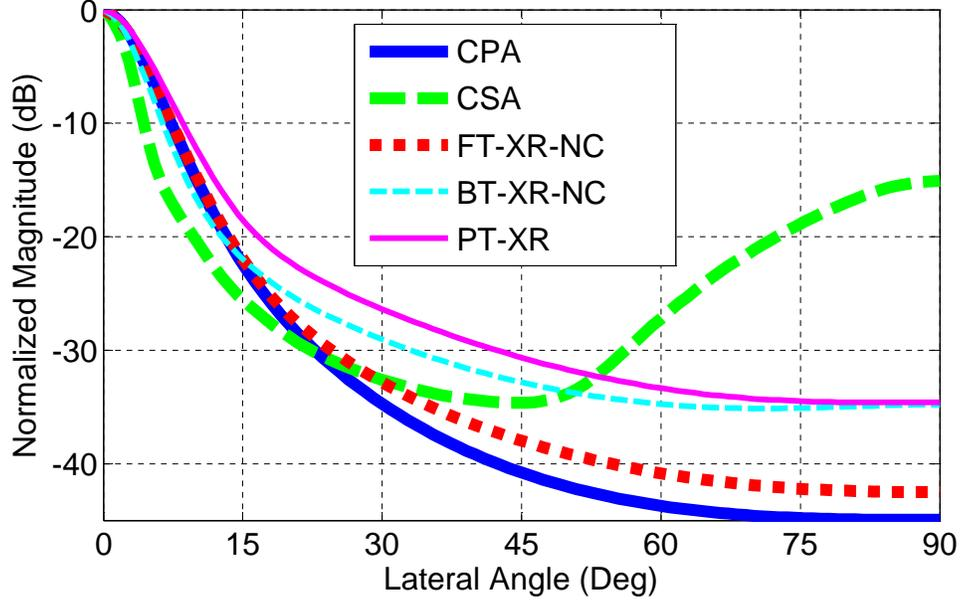


Figure 5. The 1D compounded lateral PSF comparing main lobe and side lobe energies. The horizontal axis gives the spherical coordinate (Φ), the angle from the array normal. The compounding corresponds to integrating the PSF over all ρ and θ for a particular spherical coordinate Φ .

Table 2. Parameters reflecting the front-end complexity and imaging performance of classical and explored array systems.

	CPA	CSA	PT-XR	BT-XR-NC	FT-XR-NC
Tx Elements	256	256	64	60	224
Rx Elements	256	256	32	28	32
Active Tx elements	256	1	64	60	224
Active Rx Elements	256	1	16	16	16
Minimum Scan Angle (90°)	23×23	-	23×23	23×23	23×23
Maximum Frame Rate	47	97	23	23	23
6-dB Beam Width (Degrees)	5.1	3.2	6	4.5	5.2
Image SNR (dB)	72	24	51	50	63
Motion Susceptibility	1	256	2	2	2

2.2. Plus-Transmit X-Receive (PT-XR)

In PT-XR, the number of active channels is reduced from CPA. Furthermore, the SNR and grating lobes are improved in comparison with CSA. However, a relatively few number of elements are used in the transmit aperture. Because SNR is proportional to the number of transmit elements and increasing the transmit element count is relatively easy with integrated electronics, a transmit aperture utilizing more elements is preferred. Another drawback of this design is that some elements are used for both transmit and receive. This overlap slightly complicates the IC design; those elements used for both transmit and receive require circuitry to protect the low voltage receive electronics from the transmit pulse.

2.3. Boundary-Transmit X-Receive with No Common Elements (BT-XR-NC)

BT-XR-NC is similar to PT-XR in that the channel count is reduced in comparison with CPA. An advantage of this design over PT-XR is that no elements are used for both transmit and receive. However apodization with

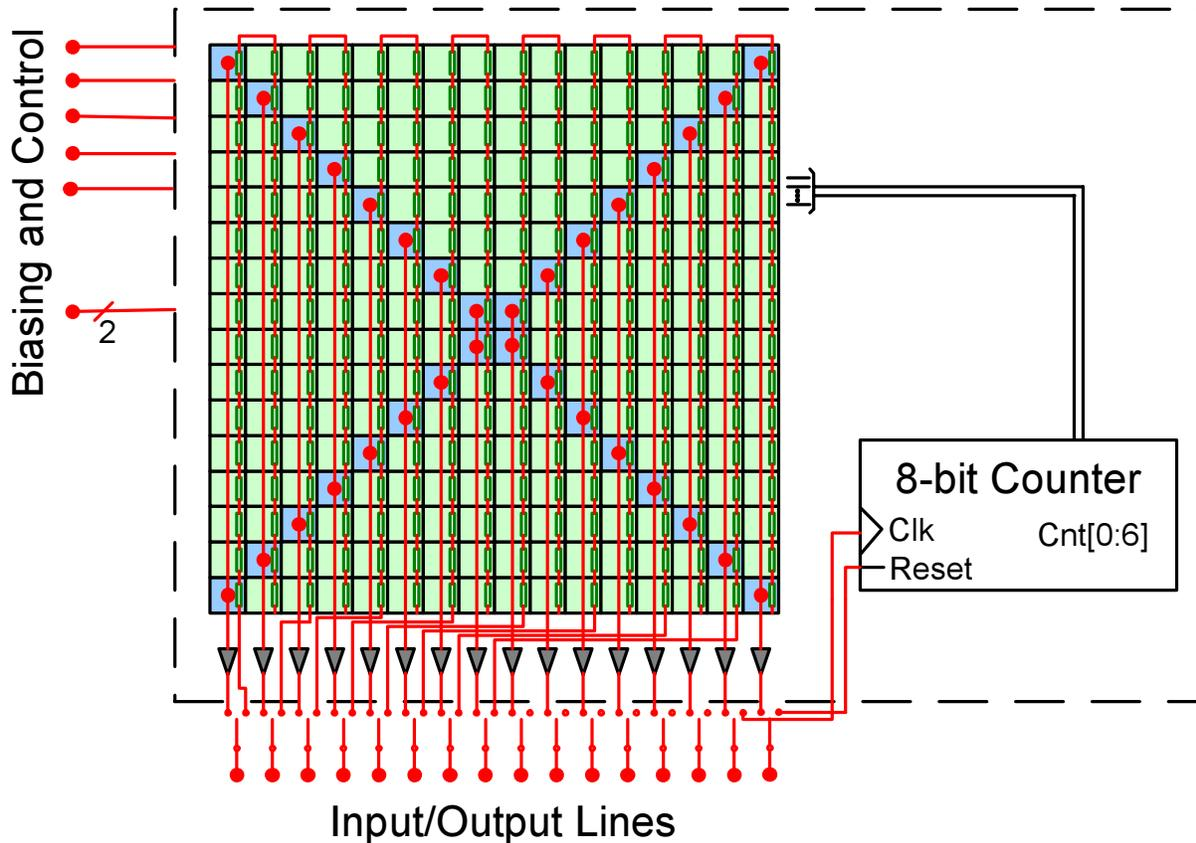


Figure 6. Architecture for an integrated circuit (IC) implementing the FT-XR-NC array design. Integrated pulsers provide 224 transmit elements. Delay information for one transmit beam is stored in memory on the IC. New delay information is loaded in the memory for each new beam. In receive, 32 receive elements are acquired with 16 receive channels.

this design is more difficult.

2.4. Full-Transmit X-Receive with No Common Elements (FT-XR-NC)

Almost the entire array is utilized on transmit in the FT-XR-NC design. Only those elements used for receive are excluded from the transmit aperture. The PSF for FT-XR-NC is comparable to the CPA PSF. The lobes seen along the diagonals of the PSF for FT-XR-NC are due to the missing elements in the transmit aperture. If the entire array is used for transmit, then a PSF even closer to that for CPA is obtained. For the imaging parameters in Table 2, the performance of FT-XR-NC approaches that of CPA and dramatically improves upon CSA. For these reasons, we have chosen this array design for the next generation of our front-end IC.

3. IC DESIGN

The architecture for an IC implementing the FT-XR-NC array design is shown in Fig. 6. A preamplifier is provided for each of the 32 receive elements. To interface to a 16-channel data acquisition system, 16 of the 32 receive elements are active at a time. Sixteen buffers drive the cable capacitance for the receive elements. A high-voltage pulser and 8-bit shift register is provided for each of the 224 transmitting elements. The timing of each pulser is determined by delay information stored in the shift register. When transmitting, a particular pulser fires when a global counter equals the pulser's stored delay value. For each new beam, delay information is loaded into the delay shift registers by 8 parallel lines. For reasonable data rates, the time required to store the delay information is a few microseconds. Thus, the frame rate is not significantly affected by the delay storage process.

4. CONCLUSION

Three array designs were evaluated for our next generation catheter-based real-time volumetric imaging system. Based on simulated PSFs, hardware complexity, SNR, and frame rate, the FT-XR-NC design was chosen for implementation. This design uses almost the entire aperture on transmit, leveraging the many transmit channels made possible by integrated electronics. Elements along the diagonals are used in receive to achieve acceptable frame rates with a 16-channel data acquisitions system. An IC implementing this design is being developed.

ACKNOWLEDGMENTS

Funding was provided by the National Institutes of Health. IC fabrication was provided by National Semiconductor. Bill Broach and the members of the Portable Power Group at National Semiconductor provided valuable process and circuit design discussions.

REFERENCES

1. R. E. Davidsen and S. W. Smith, "Two-dimensional arrays for medical ultrasound using multilayer flexible circuit interconnection," *IEEE Trans. Ultrason., Ferroelect., Freq. Cont.*, vol. 45, pp. 338-348, Mar. 1998.
2. M. I. Fuller, T. N. Blalock, J. A. Hossack, W. F. Walker, "A portable, low-cost, highly integrated, 3D medical ultrasound system," in *2003 IEEE Symposium on Ultrasonics*, vol. 1, pp. 38-41, Oct. 2003.
3. I. O. Wygant et al., "An endoscopic imaging system based on a two-dimensional CMUT array: real-time imaging results," presented at the 2005 IEEE International Ultrasonics Symposium, Rotterdam, The Netherlands, Sep. 18-21, 2005.
4. R. T. Hocter and S. A. Kassam, "The unifying role of the coarray in aperture synthesis for coherent and incoherent imaging," *Proceedings of the IEEE*, vol. 78, no. 4, pp. 735-752.
5. W. F. Walker and G. E. Trahey, "The application of k-space in pulse echo ultrasound," *IEEE Trans. Ultrason., Ferroelect., Freq. Cont.*, vol. 45, no. 3, May 1998.
6. D. H. Turnbull and F. S. Foster, "Beam steering with pulsed two-dimensional transducer arrays," *IEEE Trans. Ultrason., Ferroelect., Freq. Cont.*, vol. 38, no. 4, pp. 320-333, July 1991.
7. J. T. Yen, J. P. Steinberg, and S. W. Smith, "Sparse 2-D array design for real time rectilinear volumetric imaging," *Ultrason. Imag.*, vol. 47, no. 1, pp. 93-110, Jan. 2000.
8. E. D. Light, R. E. Davidsen, J. O. Fiering, T. A. Hruschka, S. W. Smith, "Progress in two-dimensional arrays for real-time volumetric imaging," *Ultrason. Imag.*, vol. 20, no. 1, pp. 1-15, Jan. 1998.
9. R. E. Davidsen, J. A. Jensen, and S. W. Smith, "Two-dimensional random arrays for real time volumetric imaging," *Ultrason. Imag.*, vol. 16, pp. 143-163, July 1994.
10. A. Austeng and S. Holm, "Sparse 2-D arrays for 3-D phased array imaging—design methods," *IEEE Trans. Ultrason., Ferroelect., Freq. Cont.*, vol. 49, no. 8, pp. 1073-1086, Aug. 2002.
11. J. A. Jensen, "Field: A Program for Simulating Ultrasound Systems," in *Medical & Biological Engineering & Computing*, vol. 34, supplement 1, part 1, pp. 351-353, 1996.